# Interannual Sea Level in the Northern and Eastern Indian Ocean

ALLAN J. CLARKE* AND X. LIU

*Oceanography Department, The Florida State University, Tallahassee, Florida*

(Manuscript received 25 January 1993, in final form 7 September 1993)

ABSTRACT

Monthly Indian and Pakistani sea level records, adjusted for the effect of atmospheric pressure, were used to examine interannual sea level variability in the northern Indian Ocean. The interannual sea level is correlated along the boundary. The observations hint that interannual sea level propagates along the boundary, but the evidence is not conclusive. Calculations with the Comprehensive Ocean–Atmosphere Data Set wind stress as input to a simple model suggest that the interannual sea level signal occurs along more than 8000 km of Indian Ocean coastline extending from southern Java to Bombay and is generated remotely by zonal interannual winds blowing along the equator.

The eastern Indian Ocean boundary is broken between Indonesia and Australia and examination of northwestern Australian interannual sea level shows that it is not well correlated with that in the northern Indian Ocean. The northwestern Australian sea level is larger in amplitude, related to ENSO, and of Pacific origin. Calculations using a simple model and The Florida State University wind stress suggest that the northwestern Australian sea level is generated by zonal ENSO wind stress in the equatorial Pacific. A weighted difference between the northern Indian Ocean and southeastern Indian Ocean sea levels provides a revised estimate of the interannual upper-ocean transport of water between the two oceans. The average amplitude of this interannual transport is about 2.5 Sv (Sv $\equiv 10^6$ m$^3$ s$^{-1}$), which is smaller than estimates of 5–16 Sv for the mean transport. The interannual transport is correlated with ENSO, there being a tendency for flow from the Indian Ocean and into the Pacific during a warm ENSO event. The flow tends to reverse during a cold ENSO event.

## 1. Introduction

While much has been learned about Pacific interannual sea level variability, less is known about interannual sea level variability in the northern Indian Ocean. Perigaud and Delecluse (1993) have discussed Indian Ocean sea level variability recently using Geosat satellite altimeter data and sea level calculated using a reduced gravity model, but the observations were noisy and 4½-year long records were short for interannual analysis. Do northern Indian Ocean sea levels vary strongly interannually? Are they correlated with the ENSO signal seen along the western Australian coast (Pariwono et al. 1986)? Are they forced at the coast or remotely in the ocean interior? We seek to answer these questions using coastal Indian Ocean sea level, wind stress data, and dynamical analysis.

Following a description of the data in section 2, we discuss the main features of the northern Indian Ocean interannual sea level observations in section 3 and their dynamics in section 4. A comparison with the southeastern Indian Ocean sea level along Australia's northwestern coast and a calculation of the interocean interannual transport of water are given in sections 5 and 6. A final section contains some concluding remarks.

## 2. Data

The northern Indian Ocean sea level stations used in this study are shown in Fig. 1, while data record lengths and data sources are given in Table 1. Seven stations cover a coastline distance of about 3600 km. Other monthly sea level records were available, most notably the nearly 50-year record at Ko Taphao Noi (7.83°N, 98.43°E) located in Thailand on the eastern Indian Ocean boundary and the 50-year record at Calcutta (88.3°E, 22.55°N). But the Calcutta record is influenced by river flow and the Ko Taphao Noi record was of doubtful quality, so these and other shorter and/or suspect and/or too gappy records were not used.

Table 1 and Fig. 1 also document the atmospheric pressure data. These data are necessary for our analysis because the dynamically relevant subsurface pressure near the water surface is the sum of the pressure due to the measured sea level and the fluctuating atmospheric pressure. At some sea level stations, atmospheric pressure data are not available. However, plots of the atmospheric pressure for each station (see Fig. 2) show that it has an amplitude of only about 25% of that of the sea level and that there is very little vari-

* Also the Sea Level Center, The Florida State University.

*Corresponding author address:* Dr. Allan J. Clarke, Department of Oceanography (3048), The Florida State University, Tallahassee, FL 32306-3048.

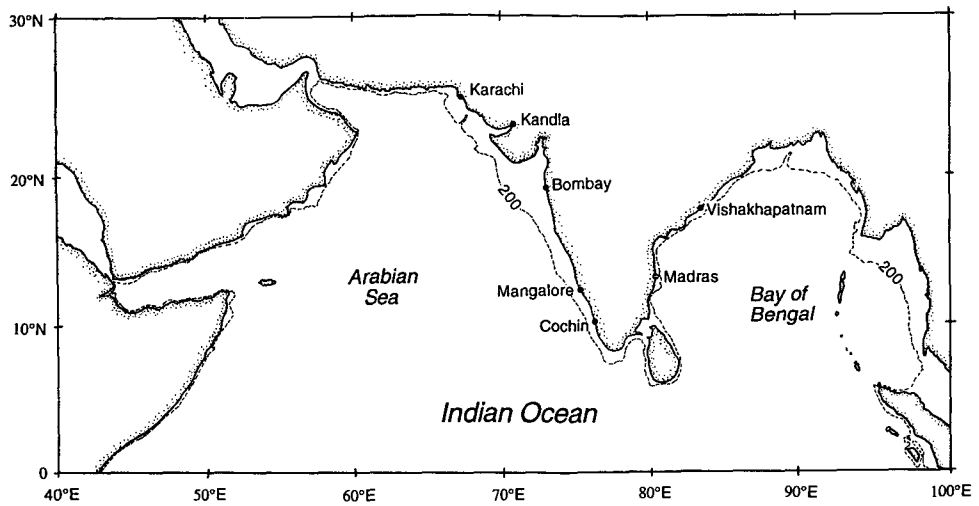


FIG. 1. Northern Indian Ocean basin. The dashed line denotes the 200-m isobath. The seven towns where sea level records were used are marked.

ation along the boundary. Since the atmospheric pressure record at Bombay is the longest, we used it to adjust the pressure at all seven sea level stations.

## 3. Northern Indian Ocean interannual sea level

To obtain the interannual sea level, each monthly adjusted sea level time series was demeaned, detrended, and filtered twice with a 13-month running mean (Chelton and Davis 1982). Gaps were treated as suggested by Mitchum (1987, personal communication). When gaps occur, they are given zero weight in the filter weighting function and the total weighting is appropriately renormalized. In this way, sometimes gaps in the time series could be filled in. A criterion is available for determining when the interpolated point is likely to be inaccurate so that the point can be flagged as missing. Based on Mitchum's analysis, we flagged an interpolated point as missing if the sum of the absolute value of the filter weights for the gap points was greater than 0.25.

Figure 3 shows the interannual sea level records from the seven sea level stations in the northern Indian Ocean. Several of the stations are visually correlated with Vishakhapatnam, and this is confirmed in Fig. 4, which shows lagged correlation with distance along the boundary from that place. Based on Chelton (1983), all stations except Mangalore are significantly correlated with Vishakhapatnam at zero lag at the 90% significance level but only Madras and Bombay are significantly correlated with Vishakhapatnam at zero lag at the 95% significance level (see Table 2). At maximum correlation, Madras *leads* Vishakhapatnam by 1 month and Bombay *lags* Vishakhapatnam by 2 months. These lags correspond to an alongshore propagation of about 26 cm $s^{-1}$ northward from Madras to Vishakhapatnam and 50 cm $s^{-1}$ from Vishakhapatnam to Bombay. However, the maximum corre-

TABLE 1. List of the station names, locations, data types, record lengths, and data sources for the data used in this study. The Permanent Service for Mean Sea Level (PSMSL) provided the monthly sea level. The National Center for Atmospheric Research provided the monthly atmospheric pressure as part of the World Monthly Surface Climatology (WMSC) dataset.

| Station | Location | Record type | Record length | Data source |
|---|---|---|---|---|
| Vishakhapatnam | 17.48°N, 83.21°E | monthly sea level | 1937–1987 | PSMSL |
| Madras | 13.08°N, 80.15°E | monthly sea level | 1952–1987 | PSMSL |
| Cochin | 9.58°N, 76.19°E | monthly sea level | 1939–1987 | PSMSL |
| Mangalore | 12.53°N, 74.52°E | monthly sea level | 1953–1987 | PSMSL |
| Bombay | 18.55°N, 72.52°E | monthly sea level | 1922–1987 | PSMSL |
| Kandla | 23.00°N, 70.20°E | monthly sea level | 1950–1987 | PSMSL |
| Karachi | 24.59°N, 68.56°E | monthly sea level | 1957–1987 | PSMSL |
| Vishakhapatnam | 17.48°N, 83.21°E | monthly atmospheric pressure | 1941–1988 | WMSC |
| Madras | 13.08°N, 80.15°E | monthly atmospheric pressure | 1941–1988 | WMSC |
| Mangalore | 12.53°N, 74.52°E | monthly atmospheric pressure | 1941–1988 | WMSC |
| Bombay | 18.55°N, 72.52°E | monthly atmospheric pressure | 1921–1988 | WMSC |

lations differ little from those at zero lag so it is difficult to be sure that "propagation" really occurs. We discuss likely dynamical reasons for the correlation and propagation in the next section.

## 4. Dynamics

Consider first frictionless unforced interannual motion near the eastern Indian Ocean boundary from the equator to the northern tip of the Bay of Bengal (see Fig. 1). Motion is geostrophic at these frequencies, so, by the condition of no normal flow into the boundary, we would expect pressure (and hence sea level) to be constant along the boundary. More precisely, at these low frequencies motion is well equatorward of the critical latitude for coastal trapping and the motion is in the form of long westward propagating Rossby waves that are in phase at the coast and have nearly constant amplitude along the boundary [for a physical discussion and documentation of critical latitudes see Clarke and Shi (1991)]. The Rossby wave signal propagates westward to the eastern coast of India, and, if the frequency is low enough, will reach it nearly in phase. In such a case pressure is approximately constant along the eastern coast of India; therefore, there is no mass flux onto the boundary and no interannual western boundary current generated. Consequently there is no interannual jet at the southern tip of the Indian subcontinent, and coastal pressure and sea level are continuous around the tip. By this argument and the requirement that low frequency pressure be spatially constant along the eastern boundary of the Arabian Sea (see Fig. 1), we expect that at very low frequencies the seven measured sea levels should be highly correlated and approximately in phase all along the northern Indian Ocean boundary.

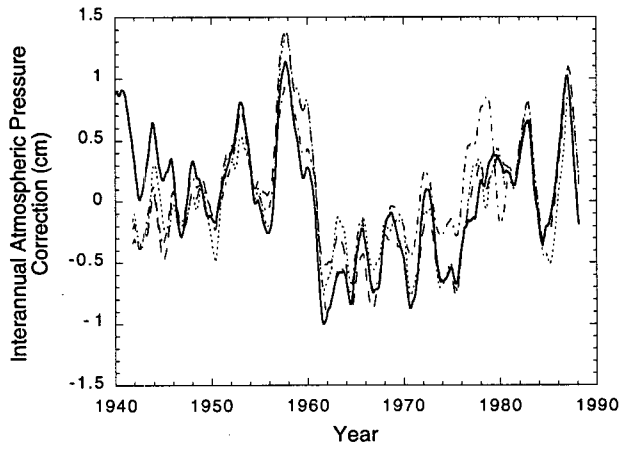


FIG. 2. Interannual atmospheric pressure correction measured in cm height of water at the four Indian coastal towns Vishakhapatnam (short dash), Mangalore (dot–dash), Madras (long dash), and Bombay (solid).

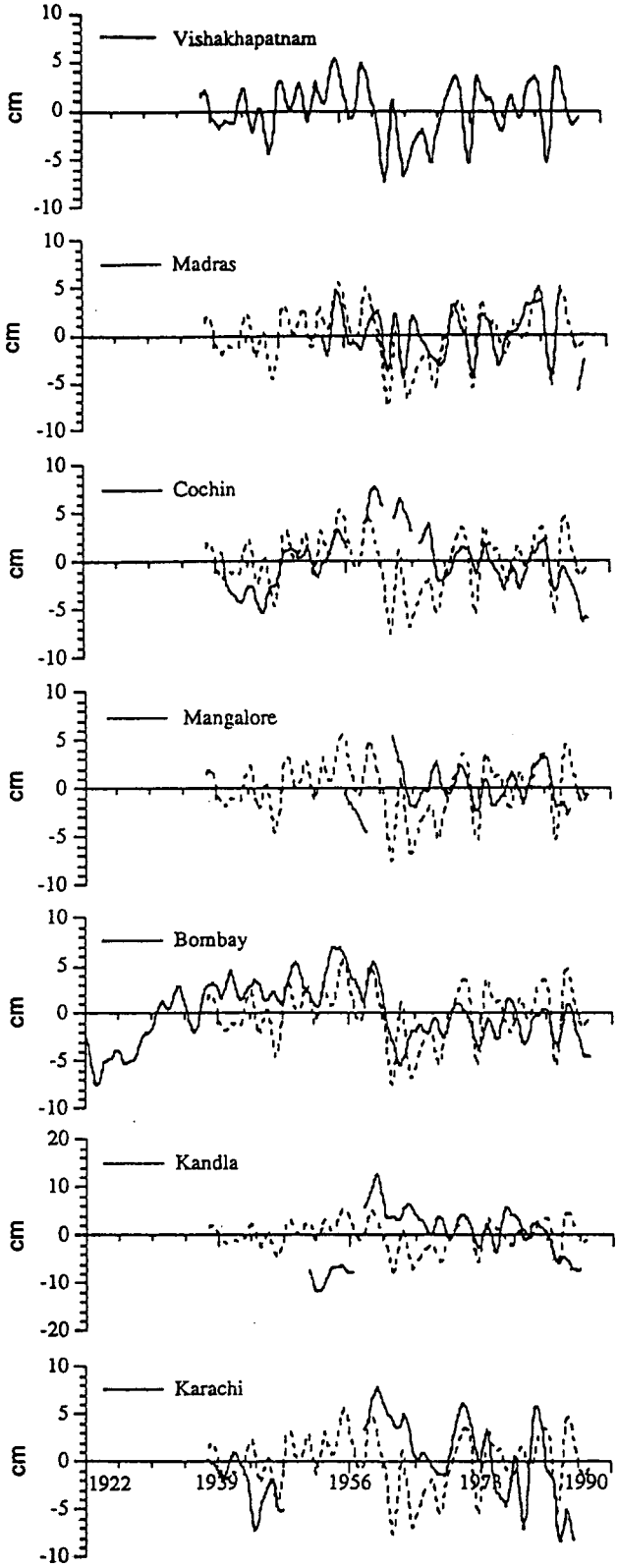


FIG. 3. Interannual sea level records from the seven sea level stations (solid lines) in the northern Indian Ocean. The Vishakhapatnam record (dashed line) has been included in the lower six plots for comparison.

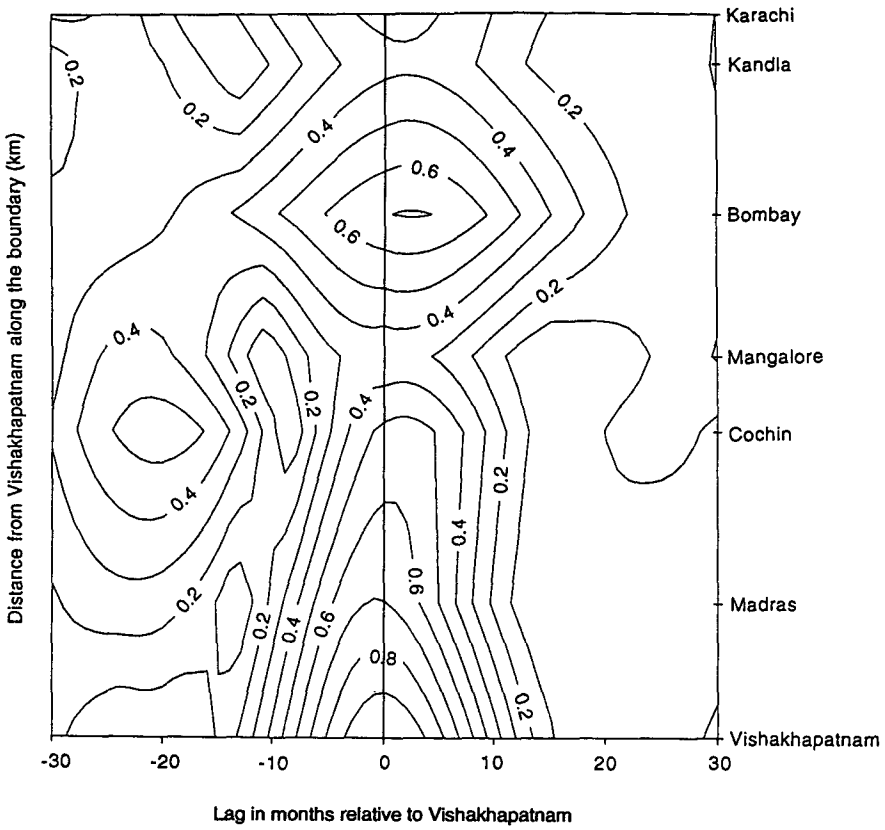


FIG. 4. Contour plot of the correlation between interannual coastal sea level in months ($t$ + lag) at each of six coastal tide gauge stations and the coastal tide gauge record at Vishakhapatnam at time $t$. Significance levels vary with station–station correlation because overlapping record lengths vary. Zero lag 90% and 95% significance levels found using Chelton (1983) are given in Table 2. The vertical line through zero marks zero lag relative to Vishakhapatnam.

While the above simple model may explain why the interannual sea level may be correlated over more than 2600 km in the northern Indian Ocean, it assumes that coastal wind forcing is negligible and does not explain how the signal is generated. Clarke (1992) showed that low-frequency sea level along an eastern ocean boundary can be described by the sum of a spatially constant boundary signal remotely generated along the equatorial waveguide and a spatially varying boundary signal forced by the coastal alongshore wind stress. How is the interannual sea level signal forced in the northern Indian Ocean case? We decided to find out by calculating interannual boundary sea level using COADS (Comprehensive Ocean–Atmosphere Data Set) monthly wind stress and the simple model of Clarke and Liu (1993). The model eastern boundary sea level is based on a simple formula given in Clarke (1992) with the remotely generated equatorial Kelvin

TABLE 2. Correlation between observed interannual sea level at Vishakhapatnam and interannual sea level at six other tide gauge stations in northern India. The significance levels were calculated using the analysis of Chelton (1983).

| Stations | Alongshore distance from Vishakhapatnam (km) | Correlation between observed sea levels and sea level at Vishakhapatnam | 90% significance level | 95% significance level |
|---|---|---|---|---|
| Madras | 680 | 0.70 | 0.48 | 0.54 |
| Cochin | 1530 | 0.53 | 0.50 | 0.57 |
| Mangalore | 1910 | 0.32 | 0.38 | 0.44 |
| Bombay | 2610 | 0.69 | 0.59 | 0.66 |
| Kandla | 3360 | 0.37 | 0.34 | 0.40 |
| Karachi | 3610 | 0.42 | 0.40 | 0.46 |

wave signal being found from forced equatorial wave theory along the lines of Gill and Clarke (1974). The model determines the sea level response with only the first two baroclinic vertical modes since only these contribute significantly to sea level. S. Levitus kindly provided the buoyancy frequency data to calculate the vertical modes. In the calculations, friction and dissipation were set to zero.

Our results indicated that indeed the interannual coastal alongshore wind stress forcing was negligible so that the calculated sea level signal was very nearly spatially constant along the boundary (see Fig. 5). This should be a robust result since it depends only on the alongshore wind stress data being approximately correct in magnitude rather than being accurate in detail.

Model and observed interannual sea level are shown in Fig. 6 for Vishakhapatnam, Madras, and Bombay. Considering that wind stress and sea level data are noisy, and that the model is linear and simple, the agreement between model and observed sea levels is quite good. Model and observed sea levels at these stations are significantly correlated at the 95% significance level (see Table 3). Table 3 also shows that other stations are less well correlated. This is probably because these stations are noisier since they are also the stations that have lower correlation between their observed interannual sea levels and Vishakhapatnam interannual sea level. In summary, these results suggest that the interannual sea level signal seen along at least 6000 km of Northern Hemisphere Indian Ocean coastline from the equator to Bombay is generated by zonal interannual winds blowing along the equator.

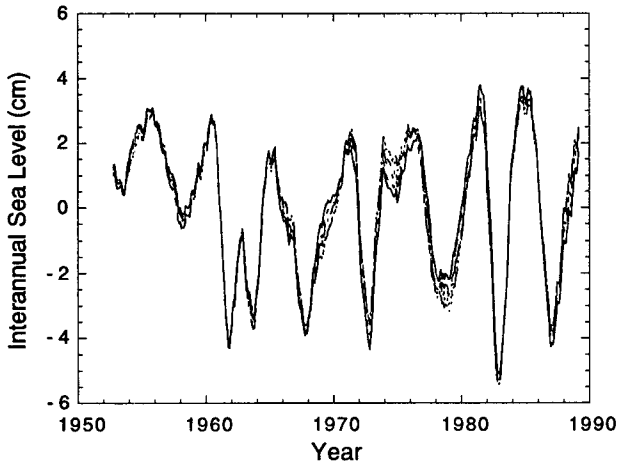


FIG. 5. Interannual sea level along the Indian/Pakistan coast using the model of Clarke and Liu (1993) with COADS wind stress. Sea level has been plotted for the seven stations Karachi (solid), Kandla (long dash), Bombay (short dash), Mangalore (long-short dash), Cochin (dot-dash), Madras (dotted), and Vishakhapatnam (triple dot-dash). Locations for these stations are given in Fig. 1. The longer vertical lines on the abscissa mark mid-January of the years 1950, 1960, . . . , 1990.

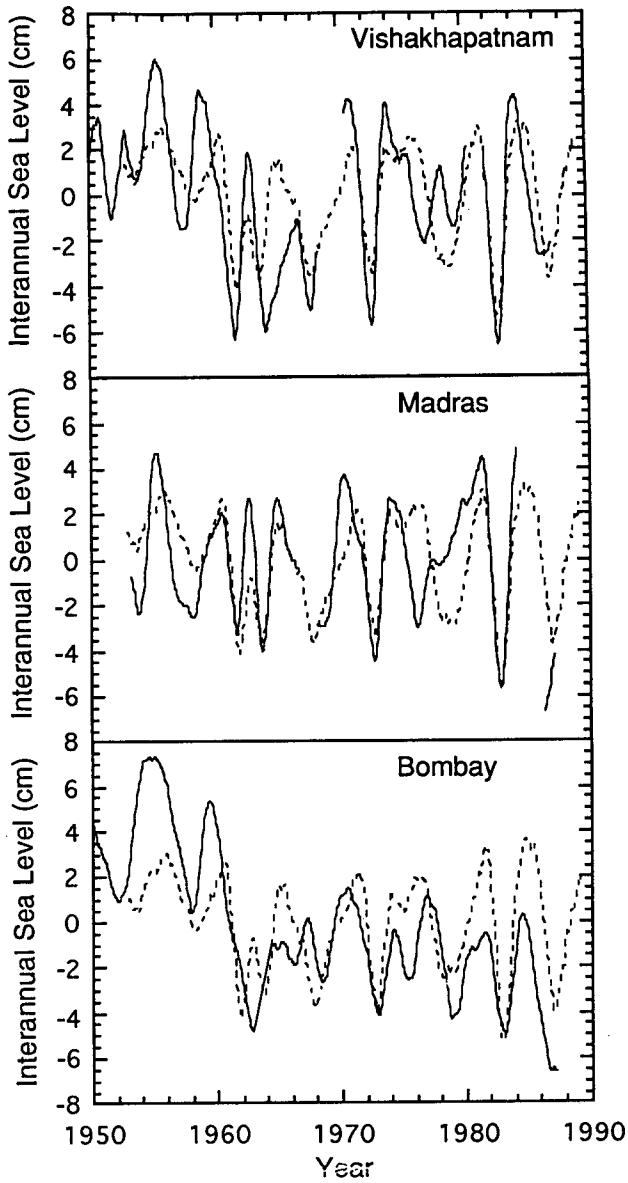


FIG. 6. Model (dashed line) and observed (solid line) interannual sea level at Vishakhapatnam, Madras, and Bombay. At each station the model and observed time series are significantly correlated at the 95% level (see Table 3). The model was based on Clarke and Liu (1993) and used COADS wind stress. The longer vertical lines on the abscissa mark mid-January of the years 1950, 1960, . . . , 1990.

The above frictionless theory predicts that the interannual sea level is in phase all along the coast. As mentioned earlier, the data hint that there is propagation along the coast, but we cannot be definite about this. Recent theory (Clarke and Van Gorder 1994) for interannual flow near an eastern ocean boundary suggests that if bottom friction and shelf and slope bottom topography are taken into account, alongshore poleward coastal sea level propagation should occur. The physics of this propagation has been described by

TABLE 3. Correlation between observed and model northern Indian Ocean coastal interannual sea level. The 95% significance level was calculated using the analysis of Chelton (1983).

| Stations | Alongshore distance from equator (km) | Correlation between observed sea levels and sea level at Vishakhapatnam | 95% significance level |
|---|---|---|---|
| Vishakhapatnam | 4010 | 0.67 | 0.55 |
| Madras | 4690 | 0.65 | 0.54 |
| Cochin | 5540 | 0.49 | 0.55 |
| Mangalore | 5920 | 0.067 | 0.46 |
| Bombay | 6620 | 0.61 | 0.55 |
| Kandla | 7360 | 0.22 | 0.38 |
| Karachi | 7620 | 0.25 | 0.38 |

Clarke and Van Gorder. Numerical calculations by them suggest that the slow northward propagation of interannual sea level along the Pacific coast of North America observed by Enfield and Allen (1980) and Chelton and Davis (1982) is explained by that physics.

What does this imply about interannual sea level for the Indian Ocean case? Along the Northern Hemisphere eastern boundary of the Indian Ocean, extending from the equator to the Ganges delta, on average interannual sea level should propagate northward at about $1/2$ to 1 m $s^{-1}$. Unfortunately there are no reliable long records to check this. All we have are data at Vishakhapatnam and Madras on the *western* boundary of the Bay of Bengal (see Fig. 1). If long Rossby waves were to propagate instantly from the eastern boundary of the Bay of Bengal to the Vishakhapatnam and Madras locations, then Madras should *lead* Vishakhapatnam. This is because the waves propagate due west and, by the Clarke and Van Gorder mechanism, sea level on the eastern boundary at the more southern latitude of Madras should lead that at Vishakhapatnam's latitude. If we take into account the finite Rossby wave speeds and the separation between the eastern and western boundaries of the Bay of Bengal at the Vishakhapatnam and Madras latitudes, we find that it takes less time for Rossby waves to cross at the Madras latitude. This again suggests that Madras should lead Vishakhapatnam. Taking into account both effects, the lead should be about 1–2 months. This is consistent with the observations although the latter are inconclusive. We also note that the theoretical arguments are also incomplete since they ignore the western boundary—the lags were essentially calculated for the points Vishakhapatnam and Madras as if they were in the open ocean.

What phase relationship should we expect between Vishakhapatnam and Bombay? By the above arguments, we may expect interannual sea level at the southern end of the Indian subcontinent to *lead* that at Vishakhapatnam, but by the Clarke and Van Gorder (1994) mechanism, sea level at Bombay should lag that at the southern end of the Indian subcontinent. Thus, we cannot definitely say, with present theoretical arguments, whether Bombay should lead or lag Vishakhapatnam.

## 5. Southeastern Indian Ocean sea level signal

The evidence and discussion in sections 3 and 4 suggest that the interannual coastal sea level signal in the northern Indian Ocean extends for over 6000 km and is generated remotely along the equator by zonal winds. Since the southern coast of Indonesia intersects the equator, we might expect that this coastline would also be influenced by a remotely generated equatorial signal. Unfortunately, no long sea level records are available along this coastline to check this hypothesis. However, calculations using COADS interannual wind stress and the Clarke and Liu (1993) model show that the effect of the alongshore coastal interannual winds on sea level is small. Therefore, the model sea level along Indonesia's southern coast is nearly the same as model sea level in the northern Indian Ocean (see Fig. 7). Based on model calculations and observed Indian sea levels, it seems that interannual sea level along a more than 8000-km stretch of coastline from southern Java to Bombay is generated remotely by zonal equatorial Indian Ocean winds.

The southeastern Indian Ocean boundary is broken between Java and Australia (see Fig. 8). How does the northwestern Australian sea level compare with that along the southern coast of Indonesia and the northern Indian Ocean? In this case data are available to answer this question. We will use a northwestern Australian sea level signal based on a combination of the Port

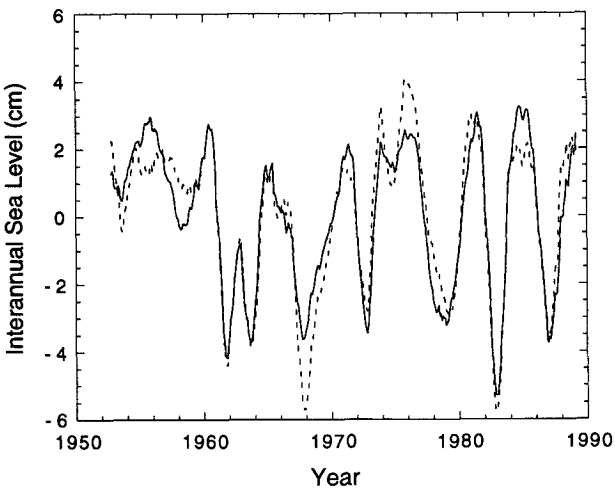


FIG. 7. Interannual sea level at Vishakhapatnam, India (solid), and Benoa, Indonesia (dashed). We calculated these time series using the model of Clarke and Liu (1993) with COADS wind stress. The locations of Vishakhapatnam and Benoa are given in Figs. 1 and 8, respectively. The longer vertical lines on the abscissa mark mid-January of the years 1950, 1960, . . . , 1990.

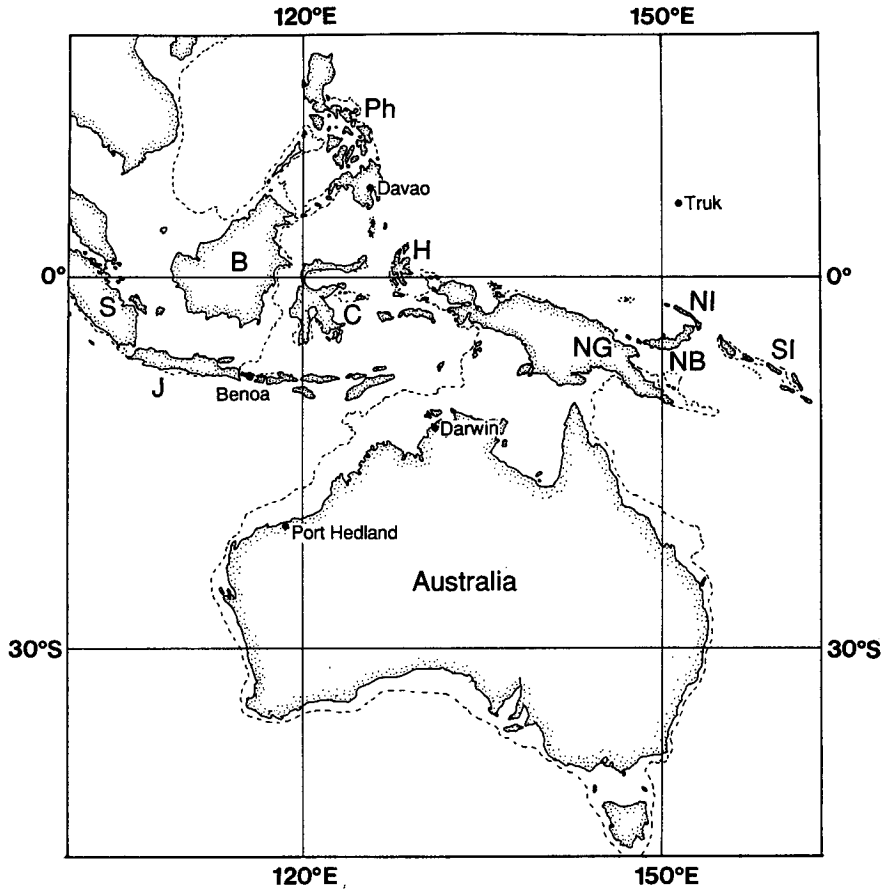


FIG. 8. The gappy western equatorial Pacific/southeastern Indian Ocean boundary region. The dashed line is the 200-m isobath. SI: Solomon Islands, NB: New Britain, NI: New Ireland, NG: New Guinea, H: Halmahera, C: Celebes, Ph: Philippines, B: Borneo, J: Java, S: Sumatra. (After Clarke 1991.)

Hedland and Darwin stations on the northwestern Australia coast (see Fig. 8) as described in Clarke (1991). Additional Australian sea level observations (Pariwono et al. 1986) show that this signal is representative of the signal along the whole southeastern boundary of the Indian Ocean and, indeed, also along the coastline as it continues around to form Australia's southern coast. In our analysis we have corrected the Darwin/Port Hedland sea level for the (small) effect of atmospheric pressure using the Darwin atmospheric pressure record.

Where does this Australian interannual sea level signal come from? Based on low frequency theory for the gappy western boundary of the Pacific, Clarke (1991) suggested that interannual Rossby wave signals generated in the interior of the equatorial Pacific would propagate westward, be largely not stopped by the Australian/New Guinea landmass and hence would influence Australia's western coast. Clarke supported his conclusion observationally by showing that the northwestern Australian signal was highly correlated with the interannual western Pacific signal at Truk Island (for location, see Fig. 8).

Another way to test whether the western Australian/southeastern Indian Ocean boundary sea level is of equatorial Pacific origin is to see if it can be calculated using equatorial Pacific wind stress. We used The Florida State University Pacific wind stress dataset (see Stricherz et al. 1992) and the forced equatorial wave model of Clarke and Liu (1993) applied to the Pacific with the western boundary condition of Cane and Gent (1984) replaced by one appropriate for the gappy western Pacific boundary. Both du Penhoat and Cane (1991) and Clarke (1991) have considered low-frequency reflection from the gappy western Pacific boundary using different models and obtained nearly identical results for the amplitude of the reflected equatorial Kelvin wave. We base our results on the Clarke (1991) model.

The equatorial Kelvin and first meridional mode equatorial Rossby waves dominate the western boundary low-frequency reflection (duPenhoat and Cane

1991; Clarke 1991) and only these were included in the Clarke and Liu forced wave model. Given the incoming first meridional equatorial Rossby wave, the reflected equatorial Kelvin wave amplitude and the western Australian pressure field can be determined for each vertical mode using Clarke's model. We used only the first two baroclinic modes in the model since these dominate the sea level response. These were summed to obtain an estimate of the interannual western Australian sea level.

A comparison of calculated and observed interannual sea level is shown in Fig. 9. The time series are visually correlated and calculations show, using Chelton (1983), that the correlation coefficient (.58) is significant at the 95% significance level (0.40). The time series satisfy the linear relation

$$\text{observed} = (0.89)\,\text{computed}, \qquad (5.1)$$

with the regression coefficient having confidence intervals ± 0.23. Thus, the predicted time series has about the same amplitude as that observed. Given the noise in the sea level data and the wind data as well as the simplicity of the theory, the results are quite good.

The above has suggested that the southeastern Indian Ocean interannual signal is of west Pacific origin and therefore is, essentially, the ENSO signal. How does this signal compare to the interannual signal in the northern Indian Ocean? Figure 10 compares the sea level at Vishakhapatnam with that at Darwin/Port Hedland. The correlation coefficient for the two time series is 0.370, which is not significant at the 95% significance level (0.41) but is at the 90% level (0.369). This weak correlation is a little surprising because although calculations show that the Java/Sumatra/Malaysia landmass extends far enough north and south of the equator to essentially block low frequency *ocean* signals, some observations have pointed to a connection between atmospheric oscillations over the two oceans (e.g., Rasmusson et al. 1990; Barnett 1983). Model Vishakhapatnam and Darwin/Port Hedland sea levels depend on zonally integrated equatorial wind stress in the Indian and Pacific Oceans, respectively, and these model sea levels are, like the observed interannual sea level, positively correlated (0.469) at the 90% significance level (0.37) but not at the 95% significance level (0.472). A positive correlation is consistent with zonal equatorial interannual wind stress in each ocean blowing in opposite directions. For example, when the zonal interannual equatorial winds in the Pacific are westerly, the zonal interannual equatorial Indian Ocean winds are easterly and sea level falls at the western Pacific and eastern Indian Ocean boundaries so that model Vishakhapatnam and Darwin sea levels both fall. This was the situation, for example, during the 1972 Pacific warm event—the interannual sea level was low in both oceans then, and Fig. 8 of Barnett (1983) shows that in September/October of 1972 Pacific equatorial winds were anomalously westerly and Indian Ocean equatorial winds anomalously easterly. But while this or its reverse also happens during other ENSO cycles, it often does not, and the sea level correlation is therefore weak.

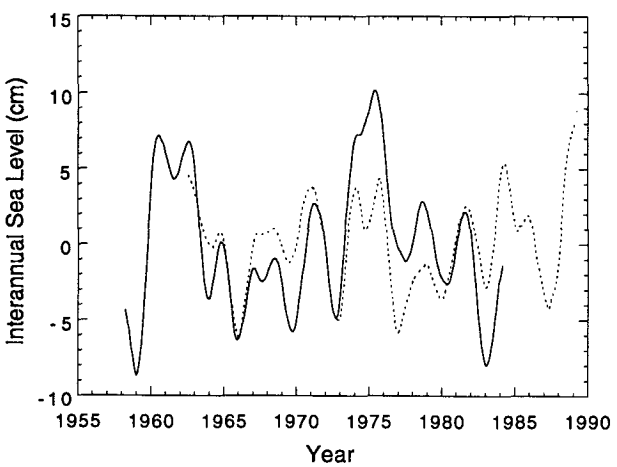


FIG. 9. Model northwestern Australian interannual sea level (dashed line) and observed (Darwin/Port Hedland) northwestern Australian sea level. Based on Chelton (1983), the time series are significantly correlated (correlation coefficient = 0.58, 95% significance level = 0.40). The longer vertical lines on the abscissa mark mid January of the years 1955, 1960, . . . , 1990.

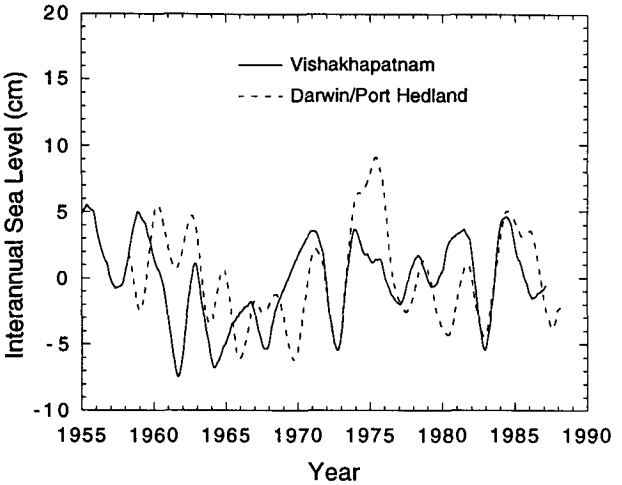


FIG. 10. Observed interannual western Australian sea level (Darwin/Port Hedland) and observed interannual sea level at Vishakhapatnam. These time series are weakly positively correlated (correlation coefficient = 0.370), significant at the 90% level (.369) but not at the 95% level (0.41). The longer vertical lines on the abscissa mark mid January of the years 1955, 1960, . . . , 1990.

## 6. Interannual transport between the Indian and Pacific Oceans

At the very low interannual frequencies of interest, Rossby wave east–west scales are very large so

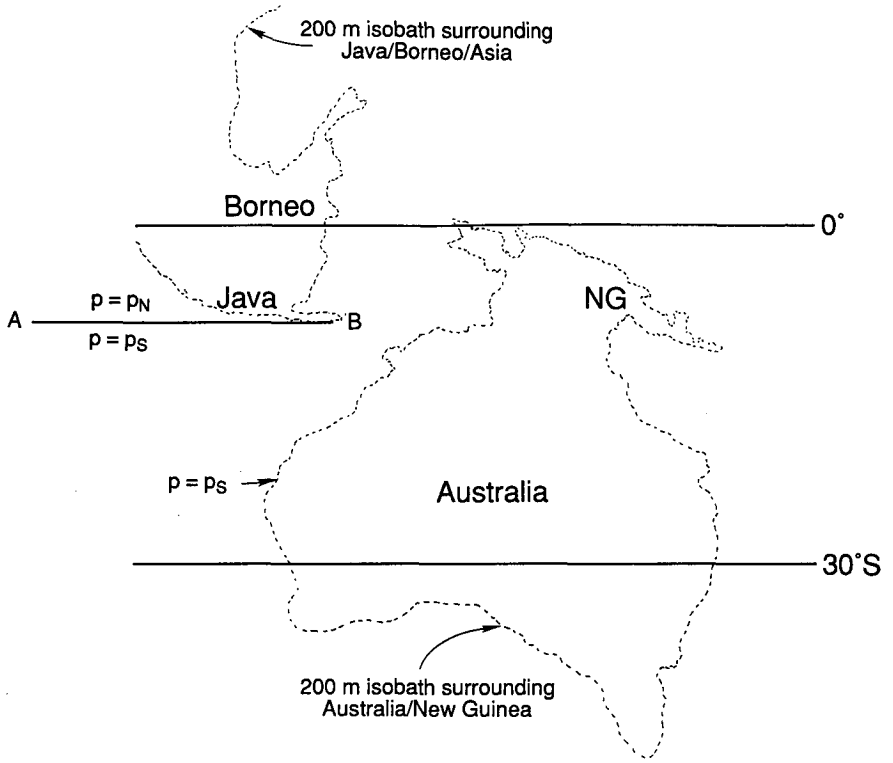


FIG. 11. Simplified version of the western Pacific boundary in which the only landmasses are New Guinea/Australia and the surrounding shelf and Indonesia/Borneo/Asia and its surrounding shelf. This simplification can be argued dynamically for flow on interannual time scales (Clarke 1991). The pressure $p_S$, west of Australia, of equatorial Pacific Ocean origin in general differs from the pressure $p_N$, west of Java and of equatorial Indian Ocean origin. This pressure difference leads to an interannual zonal flow between the oceans (after Clarke 1991).

the pressure signal $p_S$ at the western Australian coast will extend almost unchanged past the southern tip of Java (see Fig. 11). But the interannual pressure signal $p_N$ along the Java coast, being on the eastern boundary of the Indian Ocean, will be approximately equal to that at Vishakhapatnam. Since the Java and western Australian signals differ, there is an interannual pressure discontinuity and, by geostrophy, a consequent interannual flow of water between the two oceans. Because very long Rossby waves propagate east–west, the interannual flow should extend as a jet west of the southern tip of Java. In practice the jet is of finite width. Clarke (1991) has previously used such dynamics to estimate the interannual flow between the oceans but his estimate assumed that there was no Indian Ocean signal and that all of the western Australian signal was in vertical mode 1. We will revise this estimate below using an improved calculation of the interannual pressure difference.

An estimate of the upper-layer volume transport $T$ from Indian to Pacific Oceans is

$$T = \int_{-h(t)}^{0} \int_{S}^{N} u dy dz$$

$$= \int_{-h(t)}^{0} [p_S(z, t) - p_N(z, t)]/(\rho_0 f) dz. \quad (6.1)$$

In (6.1) $u$ refers to eastward velocity, $y$ to distance northward from the equator, $z$ to distance vertically upward from the ocean surface, $t$ to time, $\rho_0$ to mean water density, $f$ to the Coriolis parameter at the latitude of southern Java, $h(t)$ to the depth of the uppermost zero of $u$, $p_S$ to the pressure south of Java, $p_N$ to the pressure west and north of the southern tip of Java, and S and N to latitudes just south and north of the southern tip of Java.

Unfortunately, we cannot do the calculations in (6.1) with observed sea level since, given just sea level, we only know $p_S$ and $p_N$ at the surface $z = 0$. However, our calculations for the Indian Ocean with observed winds indicate that the pressure signal is dominated by vertical modes 1 and 2 and that these modes are in phase (see Fig. 12a) with amplitude ratio 1:2.51. Thus we estimate $p_N$ as

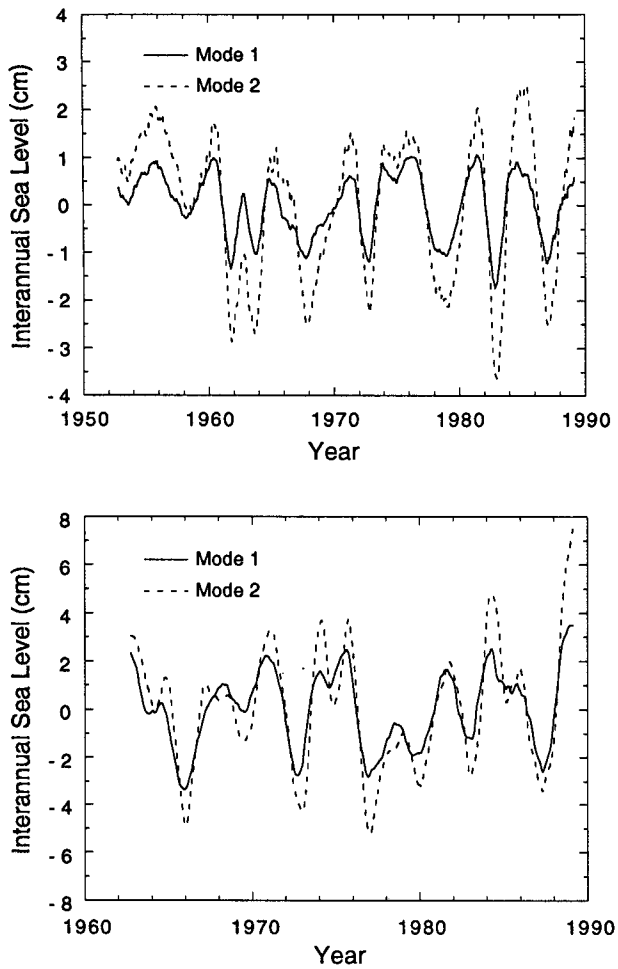


FIG. 12. (a) Interannual model sea level at the eastern Indian Ocean boundary for vertical modes 1 and 2. The modes are in phase and the rms amplitude ratio of mode 1 to mode 2 is 1:2.51. (b) Interannual model sea level along the western Australian coast for vertical modes 1 and 2. The modes are in phase and the rms amplitude ratio of model to mode 2 is 1:1.72. For both (a) and (b) the longer vertical lines on the abscissa mark mid-January of the years 1960, 1970, 1980, and 1990.

$$p_N(z, t) = \frac{1}{3.51}\left(\frac{R_1(z)}{R_1(0)} + 2.51\,\frac{R_2(z)}{R_2(0)}\right)g\eta_N, \quad (6.2)$$

where $\eta_N$ is the interannual sea level west and north of the southern tip of Java and $R_j(z)$ is the vertical mode $j$ eigenfunction. Since calculations suggest that interannual sea level is nearly spatially constant along the boundary, we will represent $\eta_N$ by the interannual sea level at Vishakhapatnam. Note that the key result that the vertical modes are in phase makes sense physically; the sea level at the eastern boundary is dominated by the vertical modes 1 and 2 equatorial Kelvin waves, and at interannual frequencies their phase does not change much in the less than 2 months time it takes them to reach the boundary from the equatorial interior.

The southern pressure $p_S(z, t)$ can also be found by using the results of the Pacific Ocean calculation described in section 5. The western Pacific equatorial ENSO signal is mainly generated in the central/west equatorial Pacific [see Fig. 16 of Kessler (1990)]. It only takes first and second vertical mode first meridional mode Rossby waves a few months to reach the boundary so we expect these to be essentially in phase when they reach the boundary. Calculations with FSU winds verify that western Pacific equatorial sea level is in phase for modes 1 and 2 (see Fig. 12b) and calculations using Clarke (1991) give (see the Appendix)

$$p_S(z, t) = \frac{1}{2.72}\left(\frac{R_1(z)}{R_1(0)} + 1.72\,\frac{R_2(z)}{R_2(0)}\right)g\eta_S, \quad (6.3)$$

where $\eta_S$ is the interannual western Australian sea level.

With these estimates of $p_S$ and $p_N$, an estimate $T$ for the upper-ocean transport from the Indian to the Pacific Ocean can be given using (6.1). The result is shown in Fig. 13. The transport $T$ is well correlated (correlation coefficient 0.80, 95% significance level = 0.61) with a transport estimate that depends solely on $p_S$ (see Fig. 13). Since $p_S$ is closely related to the western Pacific ENSO signal, we see that the transport is correlated with ENSO. Thus, when a Pacific warm event occurs, Pacific equatorial zonal winds are anomalously westerly, the western Pacific sea level falls, $p_S$ is negative and, by geostrophy, there is flow from the Indian Ocean into the Pacific. This mechanism is not always clearly apparent, however. For example, during the 1982–83 warm ENSO event, the biggest of this century, the interocean transport was near zero because zonal equatorial Pacific westerlies and zonal equatorial Indian Ocean easterlies, which often occur together (see section 5), made the sea level difference and hence

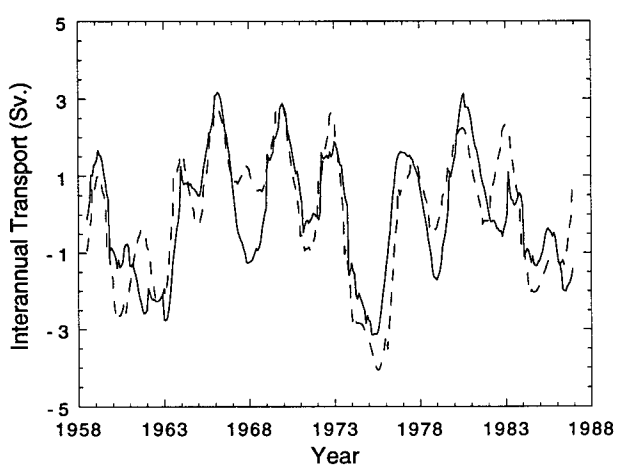


FIG. 13. Estimated [see Eq. (6.1)] interannual upper-ocean transport $T$ from the Indian to the Pacific Ocean (solid line). Also shown is the same transport calculated with Indian Ocean pressure $p_N = 0$. The longer vertical lines on the abscissa mark mid-January of the years 1958, 1963, . . . , 1988.

$|p_N - p_S|$ small. Based on this idea Wyrtki (1987) suggested that the interannual throughflow is small and unrelated to the ENSO signal. However, we find that, on average, the Pacific ENSO signal is larger than the Indian Ocean signal and that the interannual throughflow is correlated with ENSO.

Our interocean transport estimate, while qualitatively similar to Clarke (1991) in that it depends mainly on $p_S$, is smaller than his. This is mainly because two vertical modes instead of one are used to estimate the upper-ocean transport and the inclusion of the second vertical mode results in the upper-ocean depth $h(t)$ being smaller. Our mean value of $h(t)$ is 411 m and the average transport amplitude, defined $\sqrt{2}$ times the rms transport is 2.2 Sv (Sv $\equiv 10^6$ m$^3$ s$^{-1}$). This is smaller than mean transport estimates, which range from 5 to 16 Sv (Godfrey 1989).

We note that our interannual transport estimate is similar qualitatively to that obtained with the interannual transport estimate of Kindle et al. (1989). They used a global multilayer numerical model forced by the European Centre for Medium-Range Weather Forecasts 1000-mb winds to estimate the throughflow for the years 1980–1987. Their interannual transport had similar phase and amplitude to ours over the 8-year interval of overlap.

Given that our transport calculation involves differencing noisy sea levels, we decided to compare our estimated transport with that obtained from (6.1) with $p_N$ and $p_S$ directly calculated from the model using COADS (Indian Ocean) and The Florida State University (Pacific Ocean) wind stress. The transports were positively correlated but not significantly. However, they both had similar amplitudes ($\sqrt{2}$ rms = 2.6 Sv and 2.5 Sv) and were of similar character in that they were significantly correlated with the ENSO signal in the western Pacific.

## 7. Concluding remarks

Our study has suggested that the interannual sea level signal along the eastern Indian Ocean boundary, stretching more than 8000 km from southern Java to Bombay, is generated remotely by equatorial interannual zonal winds. The eastern Indian Ocean boundary is broken between Java and Australia and the northwestern Australian interannual sea level is not well correlated with that in the northern Indian Ocean. The northwestern Australian sea level is larger in amplitude, of west Pacific origin, and consequently highly correlated with ENSO. By geostrophy, the upper-ocean interannual transport of water between the Indian and Pacific Oceans can be found by subtracting an appropriately weighted difference of the interannual Java and northwestern Australian sea levels. The average interannual transport amplitude is about 2.5 Sv and has a tendency to be from the Indian to the Pacific Ocean when a warm ENSO event occurs and the west Pacific sea level is low. The transport tends to reverse for a cold ENSO event.

*Acknowledgments.* We are very thankful to Paula Tamaddoni-Jahromi for typing the manuscript and drafting many of the figures and to Bin Li for helping with Fig. 9. The National Oceanic and Atmospheric Administration funded this work under Grant NA16RCO513-01. We are grateful to various agencies and individuals for generously supplying data: PSMSL provided the northern Indian Ocean sea level, and PSMSL and the Tidal Laboratory of the Flinders Institute for Atmospheric and Marine Sciences provided the Australian sea level data (copyright reserved); Professor J. J. O'Brien at The Florida State University provided the Pacific Ocean wind stress; S. Levitus at the National Oceanographic Data Center gave the ocean buoyancy frequency, and the National Center for Atmospheric Research provided the pressure data. Contribution to the Sea Level Center, The Florida State University.

## APPENDIX

### Reflection at the Western Pacific and Western Australian Interannual Pressure

Write the northwestern Australian pressure for vertical mode $j$ as $D_j(t)R_j(z)$ and the pressure for the mode $j$ equatorial Kelvin wave leaving the western Pacific gappy boundary as

$$p = K_j(t)\psi_0(y\beta^{1/2}c_j^{-1/2})R_j(z), \qquad \text{(A1)}$$

where $\psi_0$ is the zeroth Hermite function, $\beta = df/dy$, and $c_j$ is the phase speed of the $j$th equatorial Kelvin wave. From the results of Clarke (1991),

$$\frac{D_1}{K_1} = \frac{0.595}{0.415} = 1.43,$$

$$\frac{D_2}{K_2} = \frac{0.581}{0.435} = 1.34. \qquad \text{(A2)}$$

But calculations using FSU wind stress and our Pacific equatorial model (see Fig. 12b) show that $K_2$ and $K_1$ are in phase, and, on average, have an amplitude ratio

$$K_2/K_1 = 1.84. \qquad \text{(A3)}$$

From (A2) and (A3),

$$D_2/D_1 = 1.72. \qquad \text{(A4)}$$

This result then enables us to estimate $p_S(z, t)$ in (6.3).

## REFERENCES

Barnett, T. P., 1983: Interaction of the monsoon and Pacific trade wind system at interannual time scales. Part I: The equatorial zone. *Mon. Wea. Rev.*, **111**, 756–773.

Cane, M. A., and P. R. Gent, 1984: Reflection of low frequency equatorial waves at arbitrary western boundaries. *J. Mar. Res.*, **42**, 487–502.

Chelton, D. E., 1983: Effects of sampling errors in statistical estimation. *Deep-Sea Res.*, **30,** 1083–1103.

——, and R. E. Davis, 1982: Monthly mean sea-level variability along the west coast of North America. *J. Phys. Oceanogr.*, **12,** 757–784.

Clarke, A. J., 1991: On the reflection and transmission of low-frequency energy at the irregular western Pacific Ocean boundary. *J. Geophys. Res.*, **96,** 3289–3305.

——, 1992: Low-frequency reflection from a nonmeridional eastern ocean boundary and the use of coastal sea level to monitor eastern Pacific equatorial Kelvin waves. *J. Phys. Oceanogr.*, **22,** 163–183.

——, and C. Shi, 1991: Critical frequencies at ocean boundaries. *J. Geophys. Res.*, **96,** 10 731–10 738.

——, and X. Liu, 1993: Observations and dynamics of semiannual and annual sea levels near the eastern equatorial Indian Ocean boundary. *J. Phys. Oceanogr.*, **23,** 386–399.

——, and S. Van Gorder, 1994: On ENSO coastal currents and sea levels. *J. Phys. Oceanogr.*, **24,** 661–680.

du Penhoat, Y., and M. A. Cane, 1991: Effect of low-latitude western boundary gaps on the reflection of equatorial motions. *J. Geophys. Res.*, **96**(Suppl.), 3307–3322.

Enfield, D. B., and J. S. Allen, 1980: On the structure and dynamics of monthly mean sea level anomalies along the Pacific coast of North and South America. *J. Phys. Oceanogr.*, **10,** 557–578.

Gill, A. E., and A. J. Clarke, 1974: Wind-induced upwelling, coastal currents and sea-level changes. *Deep-Sea Res.*, **21,** 325–345.

Godfrey, J. S., 1989: A Sverdrup model of the depth-integrated flow for the world ocean allowing for island circulations. *Geophys. Astrophys. Fluid Dyn.*, **45,** 89–112.

Kessler, W. S., 1990: Observations of long Rossby waves in the northern tropical Pacific. *J. Geophys. Res.*, **95,** 5183–5217.

Kindle, J. C., H. E. Hurlburt, and E. J. Metzger, 1989: On the seasonal and interannual variability of the Pacific to Indian Ocean throughflow. *Proc. Western Pacific Int. Meeting and Workshop on TOGA COARE,* Nouméa, New Caledonia, SURTROPAC, 355–366.

Perigaud, C., and P. Delecluse, 1993: Interannual sea level variations in the tropical Indian Ocean from Geosat and shallow water simulations. *J. Phys. Oceanogr.*, **23,** 1916–1934.

Pariwono, J. I., J. A. T. Bye, and G. W. Lennon, 1986: Long-period variations of sea level in Australasia. *Geophys. J. Roy. Astron. Soc.*, **87,** 43–54.

Rasmusson, E. M., X. Wang, and C. F. Ropelewski, 1990: The biennial component of ENSO variability. *J. Mar. Systems,* **1,** 71–96.

Stricherz, J. N., J. J. O'Brien, and D. M. Legler, 1992: Atlas of Florida State University winds for TOGA 1966–1985. Mesoscale Air–Sea Interaction Group Technical Report, Florida State University, 261 pp. [Available from Mesoscale Air–Sea Interaction Group, Love Building, Room 023, The Florida State University, Tallahassee, FL 32306-3041.]

Wyrtki, K., 1987: Indonesian through flow and the associated pressure gradient. *J. Geophys. Res.*, **92,** 12 941–12 946.